



**HAL**  
open science

## Adaptation of the vertebral inner structure to an aquatic life in snakes: Pachyophiid peculiarities in comparison to extant and extinct forms

Alexandra Houssaye, Anthony Herrel, Renaud Boistel, Jean-Claude Rage

### ► To cite this version:

Alexandra Houssaye, Anthony Herrel, Renaud Boistel, Jean-Claude Rage. Adaptation of the vertebral inner structure to an aquatic life in snakes: Pachyophiid peculiarities in comparison to extant and extinct forms. *Comptes Rendus. Palevol*, 2019, 18 (7), pp.783-799. 10.1016/j.crpv.2019.05.004 . hal-02430856

**HAL Id: hal-02430856**

<https://hal.sorbonne-universite.fr/hal-02430856v1>

Submitted on 7 Jan 2020

**HAL** is a multi-disciplinary open access archive for the deposit and dissemination of scientific research documents, whether they are published or not. The documents may come from teaching and research institutions in France or abroad, or from public or private research centers.

L'archive ouverte pluridisciplinaire **HAL**, est destinée au dépôt et à la diffusion de documents scientifiques de niveau recherche, publiés ou non, émanant des établissements d'enseignement et de recherche français ou étrangers, des laboratoires publics ou privés.



ELSEVIER

Contents lists available at ScienceDirect

## Comptes Rendus Palevol

www.sciencedirect.com



General Palaeontology, Systematics and Evolution (Vertebrate Palaeontology)

## Adaptation of the vertebral inner structure to an aquatic life in snakes: Pachyophiid peculiarities in comparison to extant and extinct forms



*Adaptation de la structure interne vertébrale à la vie aquatique chez les serpents : particularités des pachyophiides en comparaison des formes actuelles et éteintes*

Alexandra Houssaye<sup>a,\*</sup>, Anthony Herrel<sup>a</sup>, Renaud Boistel<sup>a,b</sup>, Jean-Claude Rage<sup>c</sup>

<sup>a</sup> UMR 7179 CNRS, Département "Adaptations du Vivant", Muséum national d'histoire naturelle (MNHN), 57, rue Cuvier, CP 55, 75005 Paris, France

<sup>b</sup> IPHEP-UMR CNRS 6046, UFR SFA, Université de Poitiers, 40, avenue du Recteur-Pineau, 86022 Poitiers, France

<sup>c</sup> UMR 7207 CNRS, Sorbonne Université, Département "Origines et Évolution", Muséum national d'histoire naturelle (MNHN), 57, rue Cuvier, CP 38, 75005 Paris, France

## ARTICLE INFO

## Article history:

Received 22 March 2019

Accepted after revision 29 May 2019

Available online 15 November 2019

Handled by Michel Laurin

## Keywords:

Snake

Vertebra

Microanatomy

Aquatic lifestyle

Osteosclerosis

Pachyophiids

## ABSTRACT

Bone microanatomy appears strongly linked with the ecology of organisms. In amniotes, bone mass increase is a microanatomical specialization often encountered in aquatic taxa performing long dives at shallow depths. Although previous work highlighted the rather generalist inner structure of the vertebrae in snakes utilising different habitats, microanatomical specializations may be expected in aquatic snakes specialised for a single environment. The present description of the vertebral microanatomy of various extinct aquatic snakes belonging to the Nigerophiidae, Palaeophiidae, and Russelophiidae enables to widen the diversity of patterns of vertebral inner structure in aquatic snakes. A large-scale comparative analysis with extant snakes, including numerous semi-aquatic and aquatic forms, and additional extinct taxa, highlights that, even for snakes specialised for a single environment, vertebral microanatomy does not correlate well with the ecology. Thus, it cannot be used as a proxy for ecological inferences in snakes. In addition, the study emphasizes the strong difficulty in characterizing "osteosclerosis" in snake vertebrae. Finally, it points out and discusses the peculiarity of the marine hind-limbed snakes, the only snakes showing pachyosteosclerosis.

© 2019 Académie des sciences. Published by Elsevier Masson SAS. This is an open access article under the CC BY-NC-ND license (<http://creativecommons.org/licenses/by-nc-nd/4.0/>).

## R É S U M É

La microanatomie osseuse apparaît fortement liée à l'écologie des organismes. Chez les amniotes, l'augmentation de la masse osseuse est une spécialisation microanatomique souvent rencontrée chez les taxons aquatiques qui réalisent de longues plongées à faible profondeur. Si les travaux antérieurs ont mis en évidence le caractère plutôt généraliste de

## Mots clés :

Serpent

Vertèbre

Microanatomie

\* Corresponding author.

E-mail addresses: [houssaye@mnhn.fr](mailto:houssaye@mnhn.fr) (A. Houssaye), [anthony.herrel@mnhn.fr](mailto:anthony.herrel@mnhn.fr) (A. Herrel), [rboistel@gmail.com](mailto:rboistel@gmail.com) (R. Boistel).

<https://doi.org/10.1016/j.crpv.2019.05.004>

1631-0683/© 2019 Académie des sciences. Published by Elsevier Masson SAS. This is an open access article under the CC BY-NC-ND license (<http://creativecommons.org/licenses/by-nc-nd/4.0/>).

Mode de vie aquatique  
Ostéosclérose  
Pachyophiids

la structure interne des vertèbres chez les serpents qui se meuvent dans divers habitats, on peut s'attendre à observer des spécialisations microanatomiques chez les serpents aquatiques qui se déplacent dans un seul milieu. La présente description de la microanatomie vertébrale de divers serpents aquatiques éteints appartenant aux Nigerophiidae, Palaeophiidae et Russellophiidae permet d'élargir la diversité connue des patrons de structure interne vertébrale des serpents aquatiques. Une large étude comparative avec des serpents actuels, incluant de nombreuses formes semi-aquatiques et aquatiques, ainsi que d'autres taxons éteints, souligne que, même pour les serpents appartenant à un seul milieu, il n'y a pas de correspondance entre la microanatomie vertébrale et l'écologie. La compacité vertébrale ne peut donc pas être utilisée comme un proxy pour réaliser des inférences écologiques chez les serpents. De plus, l'étude souligne la grande difficulté qu'il y a à caractériser l'« ostéosclérose » chez les vertèbres de serpents. Enfin, elle souligne et discute la particularité des serpents marins « à pattes », les seuls à présenter une pachyostéosclérose.

© 2019 Académie des sciences. Publié par Elsevier Masson SAS. Cet article est publié en Open Access sous licence CC BY-NC-ND (<http://creativecommons.org/licenses/by-nc-nd/4.0/>).

## 1. Introduction

Extant aquatic snakes are represented within several taxa, e.g., Acrochordidae, Homalopsidae, Natricidae, Elapidae, which (non-exclusively) adapted to a great variety of freshwater and marine habitats (Ineich, 2004). Adaptation to an aquatic life occurred independently within these taxa and even several times within Elapidae (Ineich, 2004).

In addition, five extinct families of snakes adapted to various freshwater and marine environments: the Anomalophiidae, Nigerophiidae, Pachyophiidae, Palaeophiidae, and Russellophiidae. These various extinct aquatic snake taxa are known from the Cenomanian to the end of the Eocene (that is, from about 100 to 34 Myr ago).

Various adaptive features associated with an aquatic life are encountered in extant aquatic snakes, such as a permeable skin to facilitate gaseous exchange, a sublingual gland for salt excretion, a streamlined head shape minimising drag, a paddle-like tail to increase propulsion (Aubret and Shine, 2008; Babonis and Brischoux, 2012; Ineich, 2004; Segall et al., 2016, 2019). However, most of these anatomical features are not preserved in the fossil record. Conversely, one major adaptation to an aquatic lifestyle is observed in the vertebrae and ribs of the Cenomanian extinct Pachyophiidae: bone mass increase (see Houssaye, 2009; Ricqlès and de Buffrénil, 2001). In these taxa, bone mass increase consists of pachyosteosclerosis, i.e. the combination of an increase in periosteal bone deposits (pachyostosis), which confers to the bones a bloated aspect, and an increase in inner bone compactness (osteosclerosis; Houssaye, 2013). This specialization is thought to be associated with a passive control of buoyancy and body trim and it is generally encountered in poorly active swimmers performing long dives in shallow water environments (Houssaye, 2009; Ricqlès and de Buffrénil, 2001; Taylor, 2000). Pachyostosis has, however, not been mentioned for any other extant or extinct snake taxon. A high bone compactness has been documented in vertebrae of only a few extant aquatic snakes (Houssaye et al., 2013a). This raises the question of :

- whether bone mass increase, observed in many amniotes that have secondarily adapted to an aquatic life (see

Houssaye, 2009; Houssaye et al., 2016; Ricqlès and de Buffrénil, 2001 for a review), is indeed absent in these other lineages of aquatic snakes;

- how snakes differently adapted to an aquatic lifestyle in terms of their vertebral inner structure.

Vertebrae and ribs are the bones the most commonly affected by bone mass increase when it occurs (Houssaye, 2009). Moreover, vertebrae correspond to most of the snake skeleton and are the fossil snake bones the most frequently discovered. The vertebral microanatomy (i.e. the distribution of the osseous tissue in the bone) of numerous extant snakes has previously been investigated (Buffrénil and Rage, 1993; Buffrénil et al., 2008; Houssaye et al., 2010, 2013a). As for extinct snakes, data are conversely rare. They essentially pertain to pachyophiids (Buffrénil and Rage, 1993; Houssaye, 2013; Houssaye et al., 2011) and to a lesser extent to Palaeophiidae (Buffrénil and Rage, 1993; Houssaye et al., 2013b). The current study analyses the inner structure of vertebrae from several extinct snakes considered aquatic or possibly aquatic. Coupled with the addition of diverse aquatic snakes in the comparative sample of extant taxa, it will enable:

- to illustrate the occurrences of bone mass increase in aquatic snakes and to obtain a broader picture of the diversity of vertebral inner structure patterns in aquatic snakes;
- to correlate these patterns with ecological features in extant forms and to possibly make inferences about the paleoecology of the extinct snakes sampled;
- to discuss the different types of adaptation of the vertebrae to an aquatic lifestyle in snakes throughout their evolutionary history.

## 2. Material and methods

### 2.1. Material

#### 2.1.1. Fossil material

Anomalophiidae, Nigerophiidae, Palaeophiidae, and Russellophiidae are only represented by postcranial elements (Rage, 1984). Their systematic assignment was made

through vertebral characters that are diagnostic within snakes. Pachyophiidae are defined as including *Pachyophis*, *Pachyrhachis*, and all taxa more closely related to these genera than to extant snakes (Lee et al., 1999). Their status and phylogenetic position are strongly debated (Martill et al., 2015; Palci et al., 2013a, b; Reeder et al., 2015).

Concerning the fossil material, taxa from three of the five families encompassing aquatic forms were sampled (Table 1). Some data relative to Pachyophiidae are already available (Buffr enil and Rage, 1993; Houssaye, 2013). The Anomalophiidae are represented by a single species, *Anomalophis* (*Archaeophis*) *bolcensis* Auffenberg, 1959, from the lower Eocene of Italy, whose remains are scarce.

Two Nigerophiidae were sampled: the genera *Nigerophis* and *Indophis*. Nigerophiidae are known from the Cenomanian and Palaeocene of Africa and Asia. Moreover, possible nigerophiids were discovered in the latest Cretaceous of India and in the Eocene of Europe (Rage and Werner, 1999). Three preloccal vertebrae of *Nigerophis mirus* Rage, 1975a, from the Palaeocene outcrop Krebb de Sessao, in Niger, were analysed (Fig. 1). Their original position along the vertebral column cannot be determined in the absence of comparative material. The depositional milieu corresponds to a shallow marine environment (Capetta; pers. com. 2007). We also analysed four vertebrae of *Indophis sahnii* Rage and Prasad, 1992, from the Maastrichtian of Naskal, Andhra Pradesh, India. VPL/JU Unnumb.3-4 are isolated centra, so that their original position along the vertebral column cannot be determined. As for VPL/JU Unnumb.2, it is considered a posterior trunk vertebra and VPL/JU Unnumb.1 a mid-trunk one (JC. R. pers. obs.). The environment corresponds to a floodplain/brackish water (Rage et al., 2004), which is in agreement with the vertebral characters illustrating adaptation to an aquatic life (Rage and Prasad, 1992). These bones are particularly small, so that only one section per vertebra could be made (except for VPL/JU Unnumb. 2; Fig. 2). Moreover, correct sectional planes (see below) were difficult to obtain.

Within Palaeophiidae, species from the two genera *Palaeophis* (Maastrichtian–Eocene) and *Pterosphenus* (Eocene) were investigated. These snakes, which display various degrees of adaptation to an aquatic life, lived in marine or marginal marine waters (e.g., estuaries, deltas, lagoons, mangroves; Parmley and DeVore, 2005). *Palaeophis colossaeus* Rage, 1983a and *P. maghrebianus* are considered among the Palaeophiidae, and these species are thought to be less adapted to an aquatic life (Rage, 1983b). The *P. colossaeus* sections analysed, which were previously broadly described by Buffr enil and Rage (1993), were available in the collections of the MNHN. They were made from vertebrae discovered in the Lutetian of Tamaguilelt, Mali. Sections from vertebrae of *P. maghrebianus* Arambourg, 1952, from the Ypresian of the Phosphates of Morocco were previously described by Houssaye et al. (2013b). Five vertebrae assigned to *Palaeophis typhaeus* Owen, 1850 (Fig. 3), two from *Palaeophis toliapicus* Owen, 1841, and one of an undetermined *Palaeophis* species, from the Ypresian of Pr emont re, Aisne, northern France and Egem, Pittem, Belgium, were analysed. These two species are considered more highly adapted to an aquatic life than *P. maghrebianus*

(Rage et al., 2003). We also analysed two vertebrae from *Pterosphenus schucherti* Lucas, 1899, from the late Eocene of Georgia, USA. This species, assumed to have lived in estuarine or low-salinity environments (Hutchison, 1985; Westgate and Ward, 1981), is thought to be one of the most adapted to an aquatic life within Palaeophiidae (Rage et al., 2003).

As for Russellophiidae, we sampled the species *Russellophus tenuis* Rage, 1975b, from the early Eocene of France and India. The two vertebrae come from the late Ypresian of Cond e-en-Brie, Aisne, northern France. This taxon was thought to live in rivers, lakes, and estuaries (Rage, 1983b).

For comparative purposes, sections of two unnumbered vertebrae of the pachyophiid snake *Simoliophis rochebrunei* from Les Renardi eres, in Charente-Maritime, France, described in Buffr enil and Rage (1993), and three vertebrae of *Palaeophis maghrebianus* from the Ypresian Phosphates of Morocco, described in Houssaye et al. (2013b), were also analysed, but not described.

### 2.1.2. Extant taxa

Our sample includes the various semi-aquatic and aquatic extant snakes from Houssaye et al. (2013a) and additional semi-aquatic and aquatic taxa (Table 2; Fig. 4). These taxa were added in order to better represent the diverse ecologies encountered within aquatic snakes, with deep divers (e.g., *Hydrophis peronii*, *Hydrophis elegans*) and shallow swimmers (most *Aipysurus* species), the unique pelagic species (*Hydrophis platurus*), taxa occupying diverse habitats (e.g., *Hydrophis stokesii* and *Hydrophis curtus*) and others with a more specialized niche (*Emydocephalus annulatus*), live-bearers (all homalopsids) and oviparous taxa (*Laticauda* species), forms living almost exclusively in water (hydrophiids, acrochordids), and some regularly coming onto land (*Laticauda* species; Heatwole, 1999).

All vertebrae of extant taxa are mid-preloccal ones, where bone mass increase is supposed to be the most intense when it occurs (see Houssaye, 2013 for data relative to Pachyophiidae). Fossil vertebrae are all preloccal, but their position along the vertebral column is variable (see above) as the sampling choice was limited. The strongest variation in the intensity of bone mass increase in pachyophiids, however, essentially concerns pachyostosis, whereas osteosclerosis is more homogeneous along the preloccal region (Houssaye, 2013). The impact of this potential bias for compactness comparisons is therefore considered limited.

## 3. Methods

Various methods were used to investigate the vertebral microanatomy of our sample [for the material already digitized for Houssaye et al. (2013a), see details therein]. If some classical thin sections could be made for a few specimens, virtual ones, through the use of microtomography, were preferred for most specimens, especially because of the rarity of this material and the wish to use a non-destructive technique (Tables 1 and 2). Classical thin sections were made in the mid-sagittal and the neutral transverse planes using standard techniques (see Houssaye et al., 2008). However, as *Indophis* vertebrae

**Table 1**

List of the material of extinct taxa analysed. Abb.: abbreviation (used in Fig. 14); Resol: resolution (in  $\mu\text{m}$ ). All fossil specimens were scanned at the ESRF, Grenoble, France. CIs and Cts: compactness (in %) in longitudinal and transverse sections, respectively; CL: centrum length (in mm); USTL: Université des Sciences et Techniques du Languedoc, Montpellier, France; VPL: Vertebrate Palaeontology Laboratory, University of Jammu, Jammu, India; MNHN: Muséum national d'histoire naturelle, Paris, France; Unnumb.: unnumbered.

**Tableau 1**

Liste du matériel de taxons éteints analysés. Abb. : abréviation (utilisée dans la Fig. 14) ; Resol. : résolution (en  $\mu\text{m}$ ). Tous les spécimens fossiles ont été scannés à l'ESRF, Grenoble, France. CIs et Cts : compacité (en %) en coupe longitudinale et transversale, respectivement ; CL : longueur du centrum (en mm) ; USTL : Université des sciences et techniques du Languedoc, Montpellier, France ; VPL : Vertebrate Palaeontology Laboratory, University of Jammu, Jammu, Inde ; MNHN : Muséum national d'histoire naturelle, Paris, France ; Unnumb. : sans numéro.

Family	Taxon	Abb.	Age	Locality	Collection reference	Resol.	CIs	Cts	CL				
Nigerophiidae	<i>Nigerophis mirus</i>	Nm	Palaeocene	Krebb de Sessao, Niger	USTL SES 105	x	93.9	97.0	3.2				
					USTL SES 106	x	81.4	98.4	3.9				
					USTL SES 107	x	77.5	95.0	5.9				
	<i>Indophis sahnii</i>	X	Maastrichtian	Naskal, India	VPL/JU Unnumb.1	x	x	x	x				
					VPL/JU Unnumb. 2	x	x	x	2.4				
					VPL/JU Unnumb. 3	x	x	x	1.9				
Palaeophiidae	<i>Palaeophis colossaeus</i>	Pc	Lutetian	Tamaguilelt, Mali	VPL/JU Unnumb. 4	x	x	x	2.1				
					MNHN Unnumb. 1	x	x	69.8	x				
					MNHN Unnumb. 2	x	x	x	x				
					MNHN Unnumb. 3	x	54.7	x	11.0				
					MNHN Unnumb. 4	x	x	x	x				
					MNHN Unnumb. A	x	x	x	x				
	<i>Palaeophis maghrebianus</i>	Pm	Ypresian	Phosphates of Morocco	MNHN Unnumb. B	x	x	x	x				
					OCP DEK/GE 644	x	92.1	90.4	11.6				
					OCP DEK/GE 645	x	85.1	91.7	8.4				
					OCP DEK/GE 646	x	82.4	88.5	11.5				
					<i>Palaeophis typhaeus</i>	Pt	Ypresian	Prémontré, France	MNHN Unnumb. A	20.2	54.4	60.9	13.8
									MNHN Unnumb. B	20.2	73.3	86.4	12.8
									MNHN Unnumb. C	5.06	53.7	71.5	5.3
					<i>Palaeophis toliapicus</i>	Pto	Ypresian	Egem, Belgium	MNHN Unnumb. D	5.06	72.5	89.6	9.9
									MNHN CBL 8-13	5.06	52.4	73.3	8.1
MNHN CBL 3-6	5.06	70.5	85.7	6.1									
MNHN CBL 3-6	5.06	63.4	82.0	5.5									
<i>Palaeophis sp.</i>	P	Ypresian	Egem, Belgium	MNHN CBL 16					5.06	72.7	74.9	4.3	
				<i>Pterospheus schucherti</i>					Ps	Late Eocene	Georgia, USA	MNHN Unnumb. A	x
MNHN Unnumb. B	x	x	49.1	x									
Russellophiidae	<i>Russellophis tenuis</i>	Rt	Late Ypresian	Condé-en-Brie, France	MNHN Unnumb. A	5.4	82.6	99.6	3.3				
Pachyophiidae	<i>Simoliophis rochebrunei</i>	Sr	Cenomanian	Charente-Maritime, France	MNHN Unnumb. B	5.4	79.8	98.1	2.8				
					MNHN Unnumb. A	x	x	99.8	x				
					MNHN Unnumb. B	x	92.8	x	4.9				

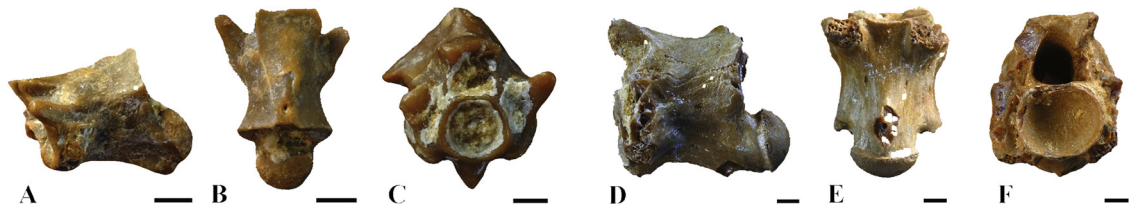


**Fig. 1. *Nigerophis mirus*.** Krebb de Sessao, Niger. Palaeocene. A–B. Vertebra USTL SES 105. C. Vertebra USTL SES 106. D–F. Vertebra USTL SES 107; in A, D, left lateral; B, dorsal; C, F, anterior; E, ventral views. The scale bars equal 1 mm.

**Fig. 1. *Nigerophis mirus*.** Krebb de Sessao, Niger. Paléocène. A–B. Vertèbre USTL SES 105. C. Vertèbre USTL SES 106. D–F. Vertèbre USTL SES 107; en vues A, D, latérale gauche; B, dorsale; C, F, antérieure; E, ventrale. Les barres d'échelle représentent 1 mm.

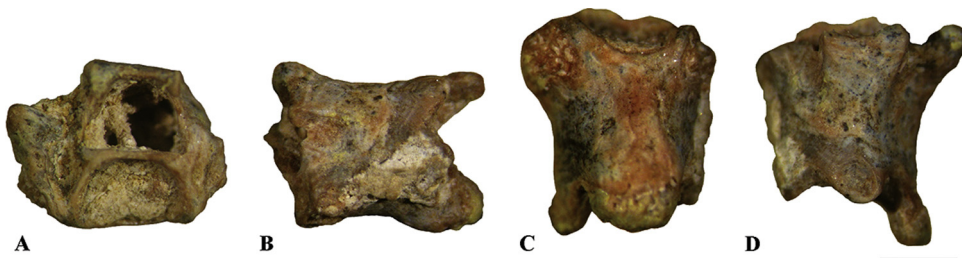


**Fig. 2. *Indophis sahnii*.** Naskal, Andhra Pradesh, India. Maastrichtian. VPL/JU Unnumb. 2 in A, anterior; B, left lateral; C, ventral; and D, dorsal views. The scale bar equals 1 mm.

**Fig. 2. *Indophis sahnii*.** Naskal, Andhra Pradesh, Inde. Maastrichtien. VPL/JU sans numéro. 2 en vues A, antérieure; B, latérale gauche; C, ventrale; et D, dorsale. La barre d'échelle représente 1 mm.

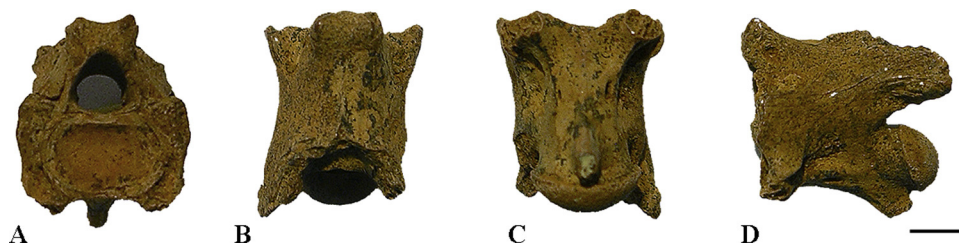


**Fig. 3.** *Palaeophis typhaeus*. Prémontré (Northern France). Ypresian. MNHN Unnumb. vertebra B in A, anterior; B, dorsal; C, ventral; D, left lateral views. The scale bar represents 5 mm.

**Fig. 3.** *Palaeophis typhaeus*. Prémontré (Nord de la France). Yprésien. MNHN Vertèbre non numérotée B en vues A, antérieure ; B, dorsale ; C, ventrale ; D, latérale gauche. La barre d'échelle représente 5 mm.

were particularly thin, only one section per vertebra could be made for three of them. High-resolution computed tomography was used for numerous extant specimens at:

- the Steinmann Institut, University of Bonn, Germany (GEphoenix|X-ray v|tome|xS 180 and 240; resolution between 7.5 and 89.9  $\mu\text{m}$ ; reconstructions performed using datox/res software);
- the Montpellier Rio Imaging (MRI; Microtomograph RX SkyScan 1076; resolution: 9.4  $\mu\text{m}$ ; reconstructions performed using NRecon software);
- the University of Poitiers, France, using a X8050-16 Viscom model (resolution: between 15.7 and 34  $\mu\text{m}$ ; reconstructions performed using Feldkamp algorithm with DigiCT software, version 1.15 [Digisens SA, France]) at the laboratory Études–Recherches–Matériaux (ERM, Poitiers, France; <http://www.erm-poitiers.fr/>).

For the fossil ones, we resorted to synchrotron microtomography on the ID 19 beamline (resolution of either 7.5 or 20.2  $\mu\text{m}$ ) at the European Synchrotron Radiation Facilities (ESRF, Grenoble, France); reconstructions were performed using the filtered back-projection algorithm with the ESRF PyHST software.

Three measurements were taken on the sections using ImageJ (Abramoff et al., 2004):

- global compactness in transverse section (*Cts*), calculated as the total sectional area minus the area occupied by cavities and the neural canal multiplied by 100 and divided by the total area minus the area occupied by the neural canal;
- global compactness of the centrum in longitudinal section (*Cl*s), calculated as the total area of the centrum minus the area occupied by cavities multiplied by 100 and divided by the total area of the centrum;
- centrum length (*CL*), considered as an indicator of size.

Welch's *t*-tests (Welch, 1947) were performed on compactness data to test for differences pending on ecological categories (semi-aquatic, aquatic, terrestrial and arboreal, fossorial).

#### 4. Description

This section describes the inner structure of the fossil vertebrae sampled. It then proposes a comparative analysis

based on data from extant snakes and extinct taxa previously described.

##### 4.1. Extinct taxa

None of the specimens analysed displays any sign of pachyostosis.

###### 4.1.1. *Nigerophis mirus*

In longitudinal sections, the relative surface occupied by primary periosteal bone varies between vertebrae (Fig. 5). Indeed, primary periosteal bone resorption is restricted to the area surrounding the neutral point (point where the centrum growth starts; sensu Buffrénil et al., 2008) in USTL SES 105 and especially USTL SES 106 (Fig. 5A) so that remodelling almost exclusively occurs in the endochondral territory. However, periosteal bone resorption is more intense in USTL SES 107, where a wide cavity occupies the core of the centrum (Fig. 5C). Compactness is generally relatively high (78% < *Cl*s < 94%). Cavities are randomly shaped so that there is no true trabecular network in the endochondral territory. In the three vertebrae, remains of calcified cartilage are important in the core of trabeculae close to the neutral point (Fig. 5D).

In transverse sections, compactness is very high (95% < *Cts* < 98%). Remodelling is extremely limited. Lacking in vertebrae USTL SES 105–106 (Fig. 5B), it is observed from the core of the centrum to the base of the neural canal in USTL SES 107.

###### 4.1.2. *Indophis sahnii*

In longitudinal sections, various patterns are observed. Some vertebrae (VPL/JU Unnumb.2-3; Fig. 6A) are very compact and show a strong inhibition of primary periosteal bone resorption. Conversely, another vertebra (VPL/JU Unnumb.4; Fig. 6B) appears highly remodelled in both endochondral and periosteal territories.

In transverse sections, vertebrae appear very compact (Fig. 6C). The neural canal is wide and surrounded by a unique layer almost exclusively consisting of primary periosteal bone, except at the base of the neural canal and around some small cavities.

###### 4.1.3. *Palaeophis colossaeus*

In most longitudinal sections, both endochondral and periosteal territories are occupied by a remodelled spongia (Fig. 7A), whereas the primary periosteal bone

**Table 2**

List of the material of extant taxa analysed in this study. Abb.: abbreviation (used in Fig. 14); EC: ecological category; SA: semi-aquatic; EA: essentially aquatic; habitat data essentially from Heatwole (1999); Ineich and Laboute (2002), Gibbons and Dorcas (2004), Murphy (2007), Pauwels and Vande Weghe (2008), and Das (2015);  $\mu$ CT:  $\mu$ CT used; M: Montpellier; P: Poitiers; B: Bonn (see Method); Resol: resolution (in  $\mu$ m). CIs and Cts: compactness (in %) in longitudinal and transverse sections, respectively; CL: centrum length (in mm).

**Tableau 2**

Liste du matériel de taxons actuels analysés dans cette étude. Abb. : abréviation (utilisée dans la Fig. 14) ; CE : catégorie écologique ; SA : semi-aquatique ; EA : essentiellement aquatique ; données sur les habitats essentiellement issues de Heatwole (1999) ; Ineich et Laboute (2002), Gibbons et Dorcas (2004), Murphy (2007), Pauwels et Vande Weghe (2008) et Das (2015) ;  $\mu$ CT :  $\mu$ CT utilisé ; M : Montpellier ; P : Poitiers ; B : Bonn (voir Méthode) ; Resol : résolution (en  $\mu$ m). CIs et Cts : compacité (en %) en coupes longitudinale et transversale, respectivement ; CL : longueur du centrum (en mm).

Family	Taxon	Abb.	EC	Habitat/Ecology	Collection reference	$\mu$ CT	Resol.	CIs	Cts	CL	
Boidae	<i>Eunectes murinus</i>	Em	SA	Freshwater	MNHN AC 1893 197	x	x	69.1	73.8	9	
					MNHN AC 1940 353	x	x	69.1	x	14.3	
					MNHN SQ-Vert 9	x	x	58	78.4	15.8	
Acrochordidae	<i>Acrochordus javanicus</i>	Aj	SA	Freshwater	MNHN SQ-Vert 14	x	x	66.8	77.5	8.4	
					AH S0004	M	9.4	48.1	56	4.3	
Viperidae	<i>Acrochordus granulatus</i>	Ag	EA	Mangrove mud flats	ZRC 2.2334	P	15.7	82.0	97.5	2.3	
					MNHN 1990 3854	x	x	68	64.3	7.5	
Grayiinae	<i>Grayia ornata</i>	Go	EA	Freshwater	AH S0006	M	9.4	60.8	x	6.3	
Natricinae	<i>Amphiesma stolatum</i>	As	SA	Freshwater	ZFMK 18169	B	8.3	58.4	95.5	4.5	
					ZFMK 74 287	B	9.2	55.8	80.8	3.9	
	<i>Afonatrix anoscopus</i>	Aa	SA	Freshwater	ZFMK 65488	B	9.1	66.8	81.1	4.1	
					AH S0010	M	9.4	67.1	89.1	2.7	
	<i>Natrix</i>	Nn	SA	Water's edge	MNHN AC 1874 535	x	x	73	x	5.3	
					ZFMK 64057	B	6.0	65.4	93	3.7	
	Homalopsidae	<i>Natrix tessellata</i>	Nt	SA	Freshwater	ZFMK 24680	B	25.7	70.9	84.1	4.0
						ZRC 2.4805	P	34.0	67.5	86.3	4.3
		<i>Myrrophis chinensis</i>	Mc	SA	Freshwater	ZRC 2.4805	P	34.0	67.5	86.3	4.3
						ZFMK 44891	x	x	70	79.9	2.9
<i>Hypsiscopus plumbea</i>		Hp	SA	Freshwater	ZRC 2.5507b	P	15.7	87.9	98.5		
					MNHN 1999 8361	x	x	78.9	87.7	3.8	
<i>Enhydriis</i>		Ee	SA	Freshwater	AH S0012	B	7.5	93.0	94.8	1.8	
					AH S0012	B	7.5	80.4	77.9	1.8	
<i>Subsessor bocourti</i>		Sb	SA	Freshwater	AH S0012	B	31.9	81.1	80.5	3.9	
					AH S0012	B	31.9	79.6	75.2	3.9	
<i>Erpeton tentaculatum</i>	Et	SA	Freshwater	AH S0012	B	31.9	89.8	89.0	3.3		
				ZRC 2.3554	P	15.7	66.6	87.2	1.4		
Elapidae	<i>Phytolopsis punctata</i>	Pp	SA	Freshwater	ZRC 2.3554	P	15.7	66.6	87.2	1.4	
					MNHN-RA-1998.8583	B	35.3	88.2	96.0	2.4	
	<i>Cerberus rynchops</i>	Cr	SA	Mangrove mud flats	ZRC 2.6411	P	15.7	84.0	98.5	2.0	
					ZRC 2.4374	P	20.8	76.5	98.9	2.4	
	<i>Homalopsis buccata</i>	Hb	SA	Freshwater	ZRC 2.3672	P	20.8	65.9	90.5	1.8	
					MNHN-RA-1912.26	B	33.2	77.4	87.6	2.8	
	<i>Bitia hydroides</i>	Bh	EA	Mangrove mud flats	ZFMK 36425	x	x	72.5	87.2	3.1	
					ZFMK 36425	x	x	66.2	74.5	2.9	
	<i>Cantorina violacea</i>	Cv	SA	Mangrove mud flats	MNHN 1990 4557	B	44.8	72.1	94.2	4.3	
					ZRC 2.2018	P	17.0	86.1	95.9	3.0	
<i>Fordonia leucobalia</i>	Fl	SA	Mangrove mud flats	MNHN-RA-1994.6997	B	36.0	61.6	87.4	3.9		
				ZRC 2.2105	P	17.0	77.0	96.1	3.1		
<i>Laticauda laticaudata</i>	Ll	EA	Marine	ZRC 2.2155	P	20.8	96.0	99.6	1.9		
				MNHN-RA-1990.4519	B	41.0	74.1	93.5	4.6		
<i>Hydrophis major</i>	Hm	EA	Marine	MNHN-RA-0.7704	B	40.2	66.9	91.0	3.6		
				MNHN 1990 4506	B	89.9	78.0	87.2	5.0		
<i>Hydrophis peronii</i>	Hpe	EA	Marine	MNHN 1990 4506	B	60.9	71.4	79.1	6.1		
				ZRC uncat	P	34.0	77.7	92.3	2.8		
<i>Hydrophis ornatius</i>	Ho	EA	Marine	MNHN-RA-0.1879	B	30.7	81.3	94.0	2.9		
				ZRC 2.2032	P	20.8	74.7	87.3	1.8		
<i>Hydrophis jerdoni</i>	Hj	EA	Marine	ZRC 2.2043	P	20.8	82.7	93.1	2.2		
				ZFMK 36436	x	x	54.9	x	2.3		
<i>Hydrophis gracilis</i>	Hg	EA	Marine	AH S0014	M	9.4	65.7	82.9	4.2		
<i>Aipysurus duboisii</i>	Ad	EA	Marine								
<i>Aipysurus eydouxii</i>	Ae	EA	Marine								
<i>Aipysurus laevis</i>	Al	EA	Marine								
<i>Hydrophis curtus</i>	Hc	EA	Marine								
<i>Hydrophis elegans</i>	He	EA	Marine								
<i>Hydrophis stokesii</i>	Hs	EA	Marine								
<i>Hydrophis schistosus</i>	Hsc	EA	Marine								
<i>Hydrophis platurus</i>	Hpl	EA	Marine								

displaying radially oriented vascular canals (like in all palaeophiids) is restricted to the ventral edge of the centrum and the upper part of the cotyle. Intertrabecular spaces are irregularly shaped and randomly oriented. They are much smaller toward the epiphyses. Global compactness indices of 57.3% and 69.4% were calculated for the two sections with a complete centrum. One longitudinal section (Fig. 7B) displays a relatively limited resorption of primary periosteal bone, so that compactness is higher.

In transverse sections, compact bone generally consists of two layers surrounding the neural canal and

the periphery of the vertebra (Fig. 7C and E). They are connected by a spongiosa that occupies most of the section. Cavities are randomly shaped and distributed. In the biggest specimens, they are much more numerous and relatively smaller than in the smallest ones, conferring a honeycomb structure (Fig. 7D), which is in agreement with the description of Buffrénil and Rage (1993). A global compactness index of 69.8% was calculated (for MNHN Unnumb. 1). In the biggest sections, remodelling is very limited at the base of the neural arch causing a sharp interruption of the structure in “double-rings enclosing a

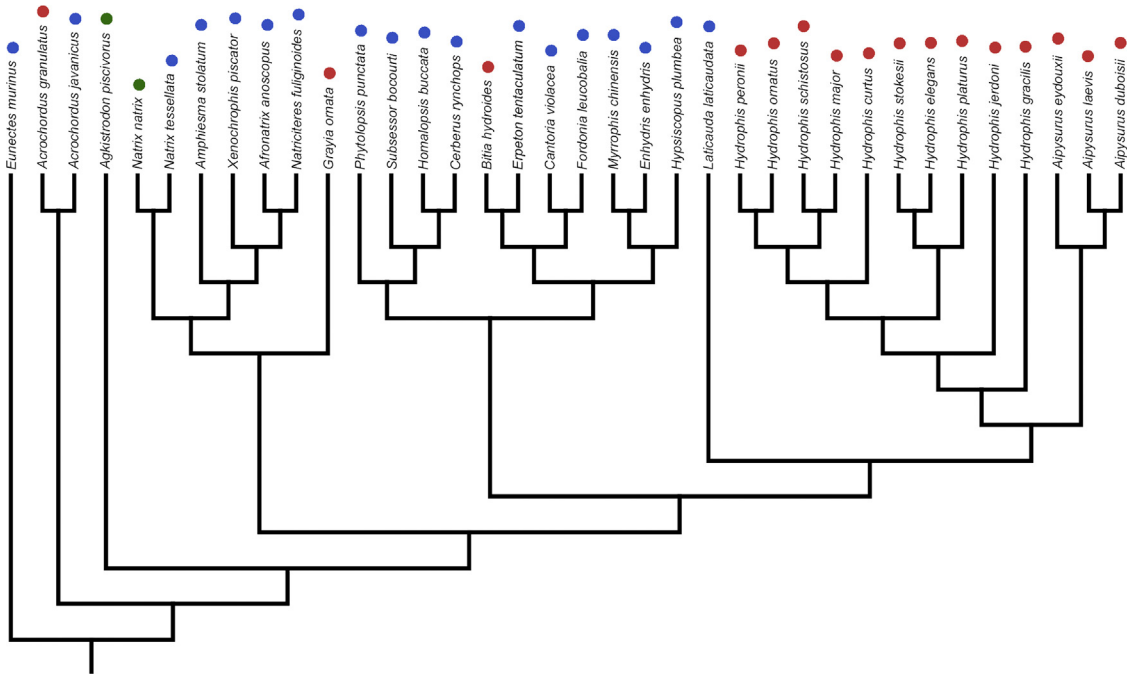


**Fig. 4.** Consensus phylogenetic tree including the extant taxa sampled, from [Figueroa et al. \(2016\)](#), with indication about their ecology: green, occasionally aquatic; blue, semi-aquatic; red, essentially aquatic.

**Fig. 4.** Arbre phylogénétique composite incluant les taxons actuels échantillonnés, d'après [Figueroa et al. \(2016\)](#), avec indication de leur écologie : vert, occasionnellement aquatique ; bleu, semi-aquatique ; rouge, essentiellement aquatique.

spongiosa" ([Fig. 7D](#)). Furthermore, one section ([Fig. 7E](#)) displays a particularly thick layer of primary periosteal bone surrounding its periphery. This section appears thus characterized by a relative inhibition of primary periosteal bone resorption.

The differences highlighted in both longitudinal and transverse sections suggest significant intraspecific and/or intracolumnar variability in this taxon.

#### 4.1.4. *Palaeophis typhaeus*

All vertebrae display a wide cavity in the core of the centrum ([Fig. 8](#)). However, the thickness of the ventral layer of compact cortex and the tightness of the spongiosa vary between the vertebrae in longitudinal section, from a thick compact cortex ([Fig. 8A](#)) to a thinner cortex surrounding a loose spongiosa ([Fig. 8C](#)). In transverse section, whereas some vertebrae show a compact neural arch and neural spine ([Fig. 8B](#)), others show a hollow neural spine sometimes associated with large cavities in the ventral part of the neural arch ([Fig. 8D](#)). As a result, some vertebrae are much more compact (MNHN Unnumb. A-B) than others (MNHN Unnumb. C-D).

#### 4.1.5. *Palaeophis toliapicus*

The structure observed in *P. toliapicus* ([Fig. 9](#)) is very similar to that previously described in *P. typhaeus*.

#### 4.1.6. *Palaeophis* sp.

This is also the case for the vertebra of *Palaeophis* sp. ([Fig. 10](#)).

#### 4.1.7. *Pterospheus schucherti*

The two longitudinal sections display similar features. Like in the other palaeophiids, a wide cavity occupies the core of the centrum, whereas the rest of the section consists of a spongiosa ([Fig. 11](#)). The latter is loose in the periosteal territory, with wide randomly shaped intertrabecular spaces, but much tighter in the endochondral territory, with relatively small numerous cavities ([Fig. 11A](#)). In transverse section, MNHN Unnumb. A displays a relatively feebly remodelled structure. Wide resorption cavities are restricted to the neural spine and the core of the centrum, whereas the rest of the section is relatively compact, with rather small and scarce cavities ([Fig. 11B](#)). Conversely, resorption is much more intense in MNHN Unnumb. B, which displays the structure in "double-rings connected by very few trabeculae" characteristic of extant squamates ([Houssaye et al., 2010](#); [Fig. 11C](#)). Compactness is thus much lower in the latter (Cts = 49.1% versus 82.5%).

#### 4.1.8. *Russellophis tenuis*

In longitudinal sections, vertebrae are highly compact (mean Cts = 81.2%). Periosteal bone remodelling appears very inhibited. There is no true trabecular network in the endochondral territory, but a few wide sub-sagittal cavities occur ([Fig. 12A–B](#)). Vascularization appears lacking in primary periosteal bone. In transverse sections, cavities are almost lacking. Compactness is thus very high (mean Cts = 98.9%). The neural canal is rather wide in this species, like in *Indophis*.



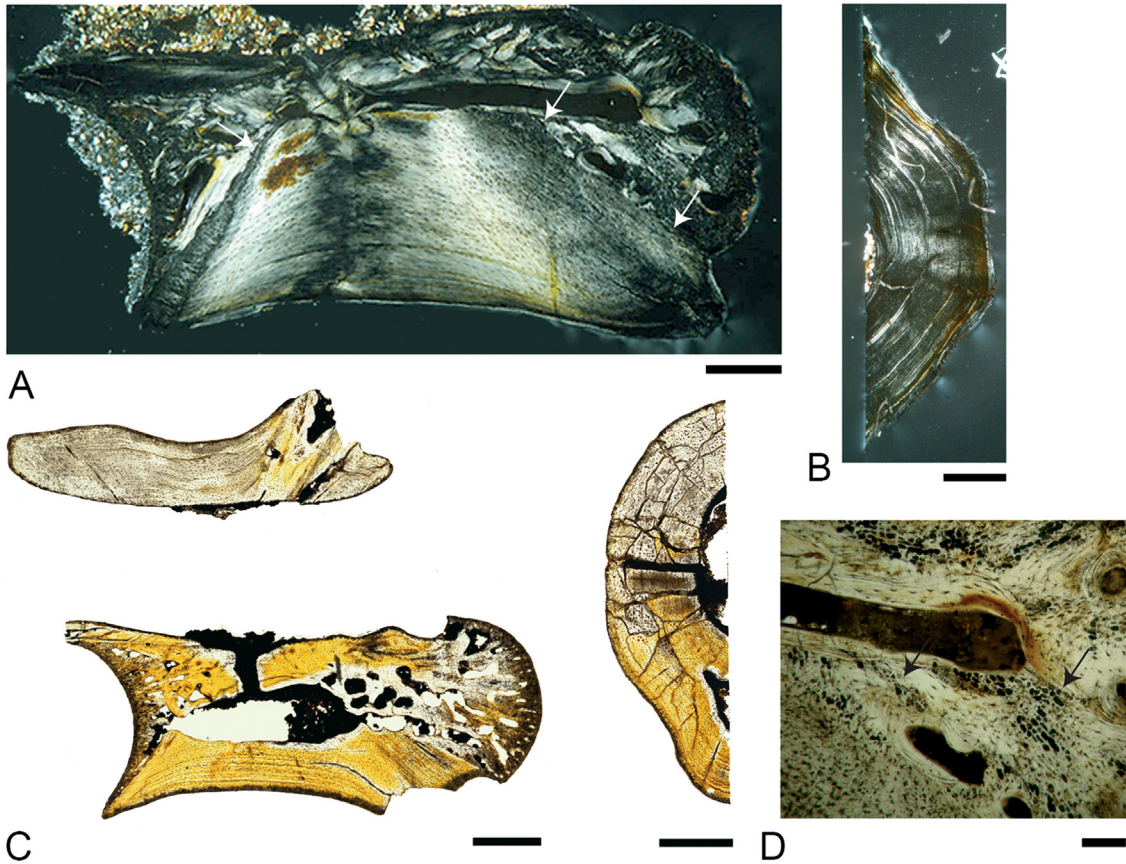


**Fig. 5.** *Nigerothis mirus*. Krebb de Sessao, Niger. Palaeocene. A, B. Vertebra USTL SES 106; A, longitudinal section (LS) of the centrum in polarized light (PL); arrows indicate the limit between periosteal and endochondral territories; B, half transverse section showing the absence of remodelling. Scale bars: 500  $\mu\text{m}$ . C, D. vertebra USTL SES 107; C, longitudinal and half transverse sections in natural light (NL); scale bars: 1 mm; D, remains of calcified cartilage (indicated by arrows) inside the trabeculae of endochondral origin in LS; scale bar: 500  $\mu\text{m}$ .

**Fig. 5.** *Nigerothis mirus*. Krebb de Sessao, Niger. Paléocène. A, B. Vertèbre USTL SES 106 ; A, coupe longitudinale (LS) du centrum en lumière polarisée (PL) ; les flèches indiquent la limite entre les territoires périostiques et endochondraux ; B, demi-coupe transversale illustrant l'absence de remaniement. Barres d'échelle : 500  $\mu\text{m}$ . C, D. Vertèbre USTL SES 107 ; C, coupes longitudinale et demi-transversale en lumière naturelle (NL) ; échelle : 1 mm ; D, restes de cartilage calcifié (pointé par des flèches) à l'intérieur des travées d'origine endochondrale en LS ; échelle : 500  $\mu\text{m}$ .

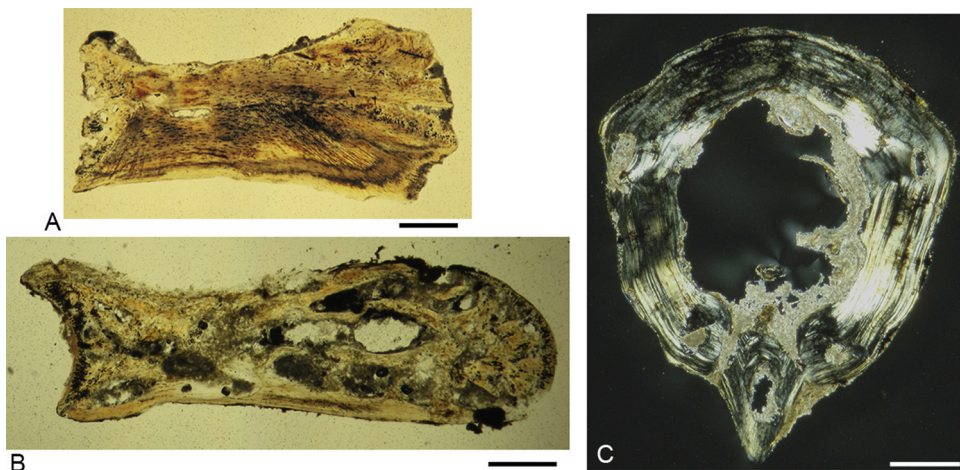


**Fig. 6.** *Indophis sahnii*. Naskal, Andhra Pradesh, India. Maastrichtian. A. VPL/JU Unnumb. 3. B. VPL/JU Unnumb. 4. C. VPL/JU Unnumb. 1 ; A–B, longitudinal sections in NL ; C, transverse section in PL. The scale bars equal 300  $\mu\text{m}$ .

**Fig. 6.** *Indophis sahnii*. Naskal, Andhra Pradesh, Inde. Maastrichtien. A. VPL/JU sans numéro. 3. B. VPL/JU sans numéro. 4. C. VPL/JU sans numéro. 1 ; A–B, coupes longitudinales en NL ; C, coupe transversale en PL. Barres d'échelle : 300  $\mu\text{m}$ .

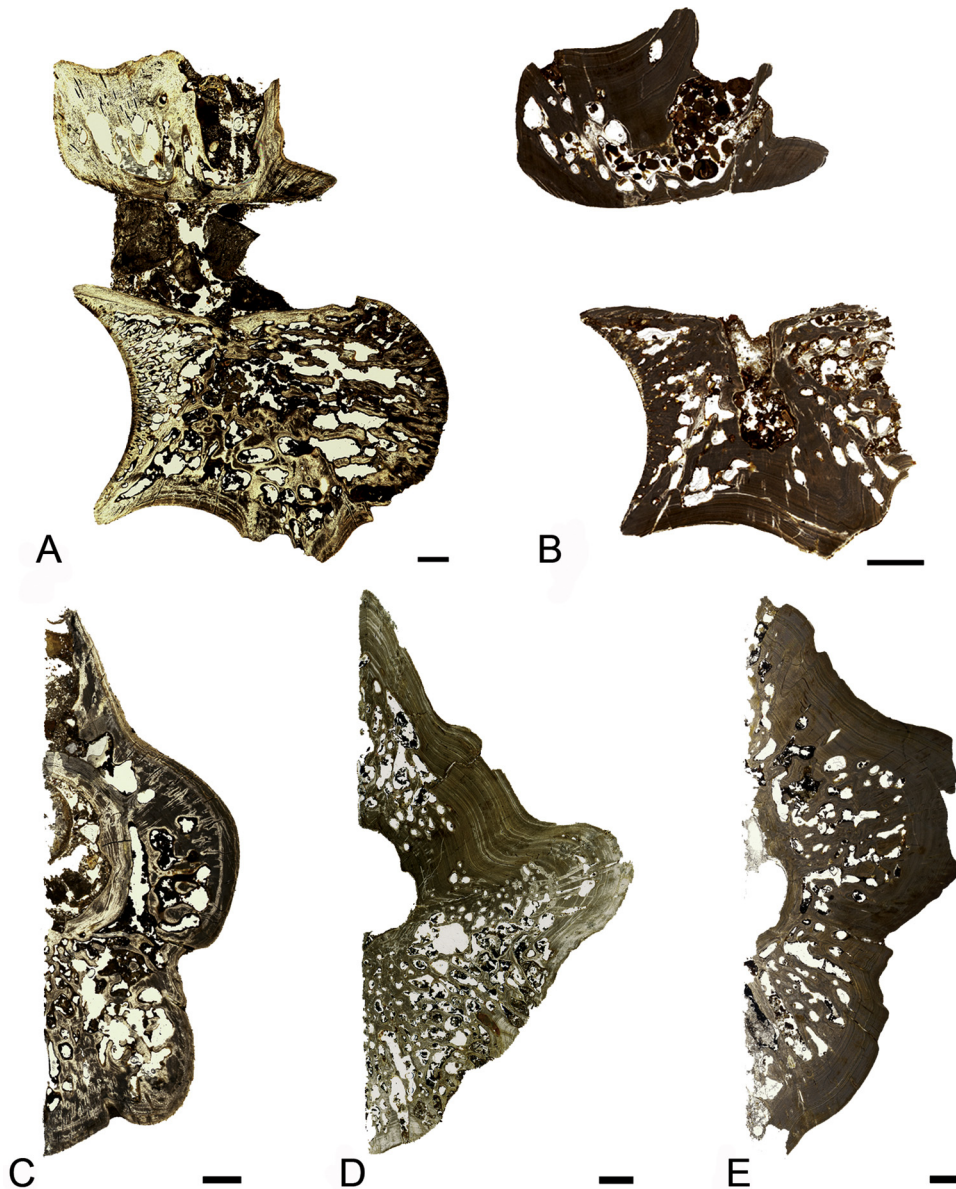


**Fig. 7.** *Palaeophis colossaeus*. Tamaguilelt, Mali. Lutetian. A–B. Longitudinal sections of A, MNHN Unnumb. 3 and B, MNHN Unnumb. A in NL. C–E. Vertebral transverse sections. A, MNHN Unnumb. 4; B, MNHN Unnumb. 1; C, MNHN Unnumb. B. The scale bars equal A, C, 1 mm, B, D, 2 mm, E, 1.5 mm.

**Fig. 7.** *Palaeophis colossaeus*. Tamaguilelt, Mali. Lutétien. A–B. Coupes longitudinales de A, MNHN Unnumb. 3 et B, MNHN Unnumb. A en NL. C–E. Coupes transversales. A, MNHN sans numéro. 4; B, MNHN sans numéro. 1; C, MNHN sans numéro. B. Les barres d'échelle représentent A, C, 1 mm, B, D, 2 mm, E, 1,5 mm.

#### 4.2. Comparisons with extant taxa

Many extant aquatic snakes display a high inner compactness. Average compactness values for the extant semi-aquatic and aquatic forms are 72.9% (*Cls*) and 86.9% (*Cts*). There are no striking differences between occasionally aquatic and semi-aquatic species on the one hand (mean *Cls* = 72.1%; mean *Cts* = 84.1%) and predominantly aquatic ones (mean *Cls* = 73.9%; mean *Cts* = 90.7%), though the difference in transverse section, made at the neutral point, indicates a higher thickness of the compact cortical bone in the latter. Calculations based on data from

Houssaye et al. (2013a) indicate lower values for terrestrial (generalist and arboreal) taxa (mean *Cls* = 71.3%; mean *Cts* = 76.5%), whereas fossorial species show high compactness values (mean *Cls* = 74.9%; mean *Cts* = 86.0%), close to those observed in aquatic snakes (Fig. 13). There is no significant difference in the compactness in longitudinal section for these four ecological categories (semi-aquatic, aquatic, terrestrial and arboreal, fossorial;  $P = 0.60$  for a Welch's *t*-test), but it is significant in transverse section ( $P < 0.001$ ).

Comparisons of the compactness values obtained for the extinct and extant taxa from our sample and *Simoliophis*



**Fig. 8.** *Palaeophis typhaeus*. Prémontré (Northern France). Ypresian. A, B. MNHN Unnumb. B. C–D. MNHN Unnumb. C; A, C, longitudinal virtual section of the centrum; B, D, transverse virtual section. The scale bars equal 1 mm.

**Fig. 8.** *Palaeophis typhaeus*. Prémontré (Nord de la France). Yprésien. A, B. MNHN sans numéro. B. C–D. MNHN sans numéro. C ; A, C, coupe virtuelle longitudinale du centrum ; B, D, coupe transversale virtuelle. Les barres d'échelle représentent 1 mm.

and *Palaeophis maghrebianus* sections (see Table 1) reveal that all fossil specimens sampled exhibit compactness indices in the range of those observed in the extant aquatic snakes (Fig. 14). Moreover, no clear distinction is observed between semi-aquatic and almost exclusively aquatic forms (Fig. 13). Palaeophiids display a wide range of compactness values with some particularly light forms and the *Palaeophis maghrebianus* specimens exhibiting rather high compactness values. *Nigerophis*, *Russelophis* and *Simoliophis* exhibit high compactness values, but they are not distinct from some extant snakes (e.g., *Enhydryis*, *Cerberus rynchops*, *Homalopsis buccata*). What is of particular interest is that these snakes display various ecologies, from mangrove mud flats for *Acrochordus granulatus*, *Cerberus rynchops*, and *Bitia hydroides*, to a purely marine lifestyle,

for *Hydrophis peronii*, *H. gracilis*, *H. elegans*, *H. schistosus*, *H. stokesii*, and *H. curtus*, through freshwater environments for *Enhydryis*, *Erpeton tentaculatum*, and *Homalopsis buccata*.

## 5. Discussion

### 5.1. Histological and microanatomical features of the extinct taxa

*Nigerophis*. Vertebrae are characterized by the inhibition of both periosteal bone and calcified cartilage resorption, which evokes osteosclerosis. Whereas vertebrae USTL SES 105–106 are considered mid-trunk vertebrae, USTL SES 107 could correspond to a more anterior trunk vertebra (JCR; pers. obs.) The variation in compactness observed between

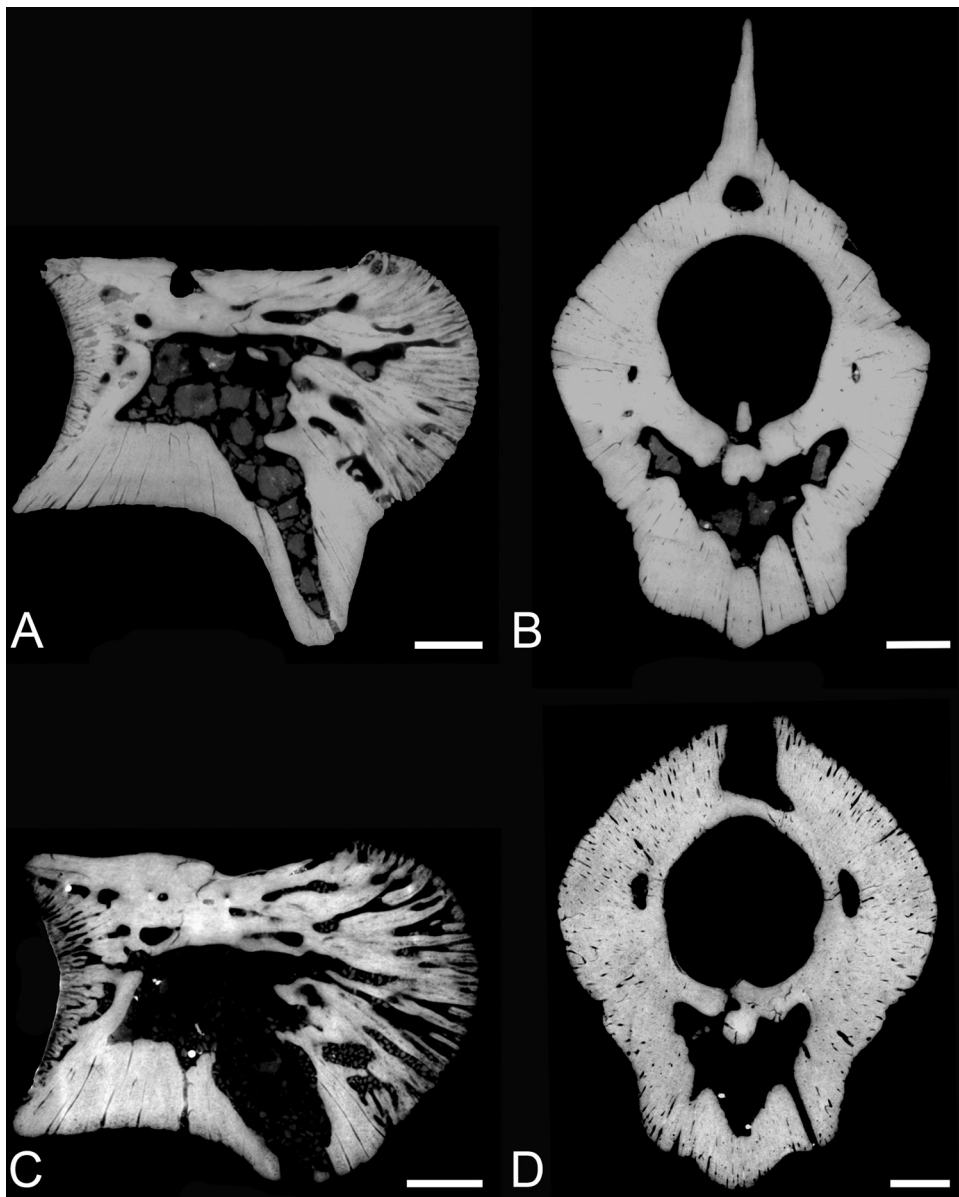


**Fig. 9.** *Palaeophis toliapicus*. Egem (Belgium). Ypresian. MNHN CBL 3-6. A, C. Longitudinal virtual section of the centrum. B, D. Transverse virtual section. The scale bars equal 1 mm.

**Fig. 9.** *Palaeophis toliapicus*. Egem (Belgique). Yprésien. MNHN CBL 3-6. A, C. Coupe longitudinale virtuelle du centrum. B, D. Coupe transversale virtuelle. Les barres d'échelle représentent 1 mm.

these vertebrae is consistent with a maximal osteosclerosis intensity in the mid-trunk region. Buffrénil and Rage (1993) described the inner organization of specimens of both *Nigerophis mirus* and *Palaeophis colossaeus* as a honeycomb weave structure characterized by an intense remodelling activity. As for *N. mirus*, this result is not in accordance with the sections analysed here. No illustration of these sections is available in the literature; however, two longitudinal sections assigned to this taxon were loaned by V. de Buffrénil. The microanatomy is relatively comparable to what is observed in vertebra USTL SES 107. Unfortunately, no cast or illustration of the original vertebrae is

available, so that no inference about the original position of these vertebrae along the vertebral column can be made.

*Indophis*. Osteosclerosis has been observed in most sections analysed, although VPL/JU Unnumb. 4 displays a pattern similar to that of most extant squamates. Osteosclerosis in this taxon is probably restricted to a peculiar region of the vertebral column that cannot be determined based on this sample.

*Palaeophiidae*. None of the *Palaeophis colossaeus* vertebrae displays osteosclerosis. Their inner structure is rather spongy. The various patterns observed show an important intraspecific variation in vertebral microanatomy. Like

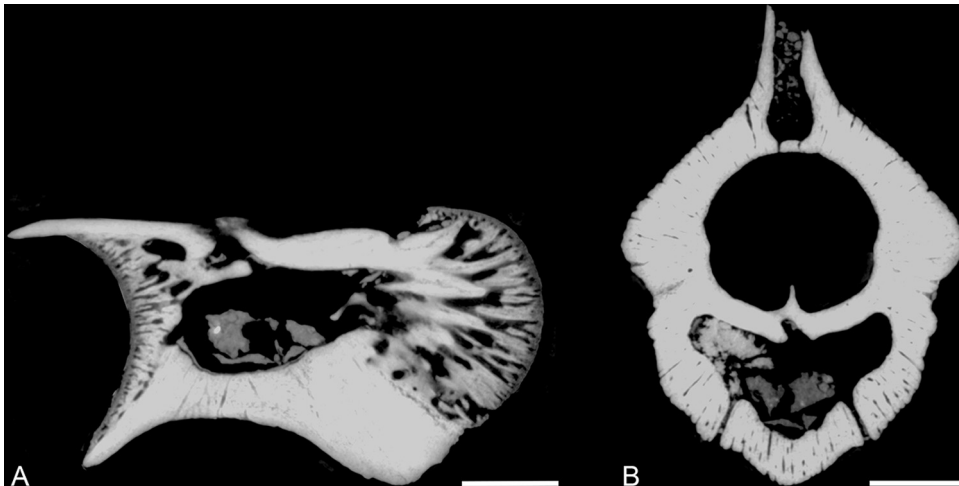


**Fig. 10.** *Palaeophis* sp. Egem (Belgium), Ypresian. MNHN CBL 16. A. Longitudinal virtual section of the centrum. B. Transverse virtual section. The scale bars equal 1 mm.

**Fig. 10.** *Palaeophis* sp. Egem (Belgique), Yprésien. MNHN CBL 16. A. Coupe longitudinale virtuelle du centrum. B. Coupe transversale virtuelle. Les barres d'échelle représentent 1 mm.

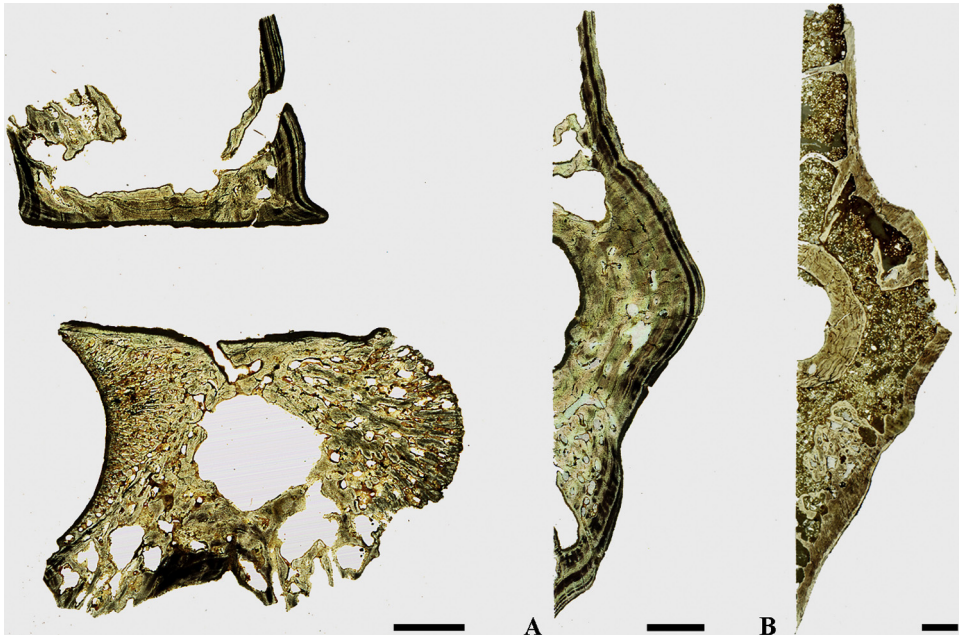


**Fig. 11.** *Pterosphenus schucherti*. Georgia, USA, Late Eocene. MNHN Unnumb. A. Longitudinal section in NL. The scale bar equals 3 mm. B–C. Half transverse sections in NL. B, MNHN Unnumb. A; C, MNHN Unnumb. B. The scale bars equal 2 mm.

**Fig. 11.** *Pterosphenus schucherti*. Géorgie, États-Unis. Éocène supérieur. MNHN sans numéro. A. Coupe longitudinale en NL. La barre d'échelle représente 3 mm. B–C. Demi-coupes transversales en NL. B, MNHN sans numéro. A; C, MNHN sans numéro. B. Les barres d'échelle représentent 2 mm.

for *P. colossaeus*, no vertebra of *Palaeophis typhaeus* displays osteosclerosis, though some vertebrae show compact neural arches and spines, whereas others do not, reflecting a rather high intraspecific variability. These vertebrae, however, all display a large central cavity in the core of the centrum. The *P. toliapicus* and *Palaeophis* sp. inner structure appears very similar to that of *P. typhaeus*. This is also the case for *Pterosphenus*. The endochondral territory in the *Palaeophis* vertebrae consists in a rather loose spongiosa, which becomes tighter in some (but not all)

of the largest vertebrae. Within Palaeophiidae, important intraspecific variation in microanatomical organization is observed, which probably reflects important intracolumnar and size variation in the vertebral microanatomy of these taxa. Further analyses on vertebrae of various sizes illustrating diverse clearly defined positions along the vertebral column would be required to explain this variability.

Most *Palaeophis* vertebrae, except those of *P. colossaeus*, show an open cavity in the core of the centrum, even

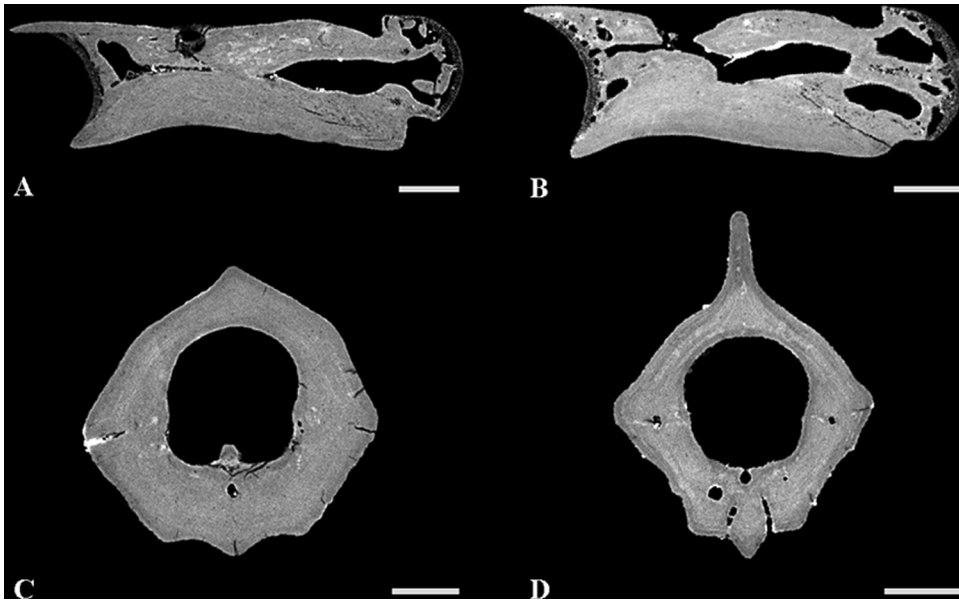


**Fig. 12.** *Russellophis tenuis*. France. Late Ypresian. A, C, MNHN Unnumb. A; B, D, MNHN Unnumb. B. A, B. Virtual longitudinal sections. C, D. Virtual transverse sections. The scale bars equal 500 μm.

**Fig. 12.** *Russellophis tenuis*. France. Yprésien supérieur. A, C, MNHN sans numéro. A ; B, D, MNHN sans numéro. B. A, B. Coupes longitudinales virtuelles. C, D. Coupes transversales virtuelles. Les barres d'échelle représentent 500 μm.

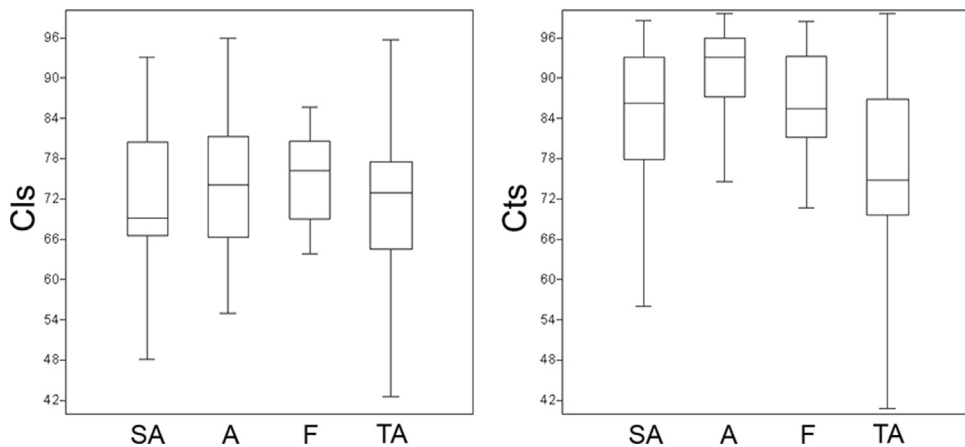


**Fig. 13.** Boxplots illustrating the differences in compactness values (Cl<sub>s</sub> in longitudinal sections; C<sub>t</sub>s in transverse sections) between extant snakes depending on their ecology; SA: semi-aquatic (n = 27 for Cl<sub>s</sub>, 25 for C<sub>t</sub>s); A: aquatic (n = 20,18); F: fossorial (n = 14,13); TA: terrestrial and arboreal (n = 34,31).

**Fig. 13.** Boîtes à moustaches illustrant les différences de valeurs de compacité (Cl<sub>s</sub> en coupe longitudinale ; C<sub>t</sub>s en coupe transversale) au sein des serpents actuels selon leur écologie ; SA : semi-aquatique (n = 27 pour Cl<sub>s</sub>, 25 pour C<sub>t</sub>s) ; A : aquatique (n = 20,18) ; F : fouisseur (n = 14,13) ; TA : terrestre et arboricole (n = 34,31).

the vertebrae of *P. maghrebianus*. This feature often occurs in snake vertebrae and even more widely in squamates (Houssaye et al., 2010, 2013a), but is not at all general to amniotes (Dumont et al., 2013; Houssaye et al., 2014).

*Russellophis tenuis*. The two vertebrae appear osteosclerotic, with only a few large cavities in the endochondral territory.

For the extinct taxa for which several specimens are available, some display rather distinct compactness values, which highlights that intraspecific variability can be high as compared to interspecific variability.

### 5.2. The occurrence of osteosclerosis

The coupled inhibitions of both calcified cartilage resorption and primary periosteal bone resorption are clearly observed in two specimens of *Nigerophis*, but only to a lesser extent in USTL SES 107, which shows a wide cavity in the core of the centrum and a compactness not particularly high. Osteosclerosis also occurs in most vertebrae of *Indopphis*, with a clear inhibition of primary bone resorption. In *Russellophis*, the observation of growth marks enables to assume a similar inhibition of primary bone resorption. However, the resolution of the virtual sections does not

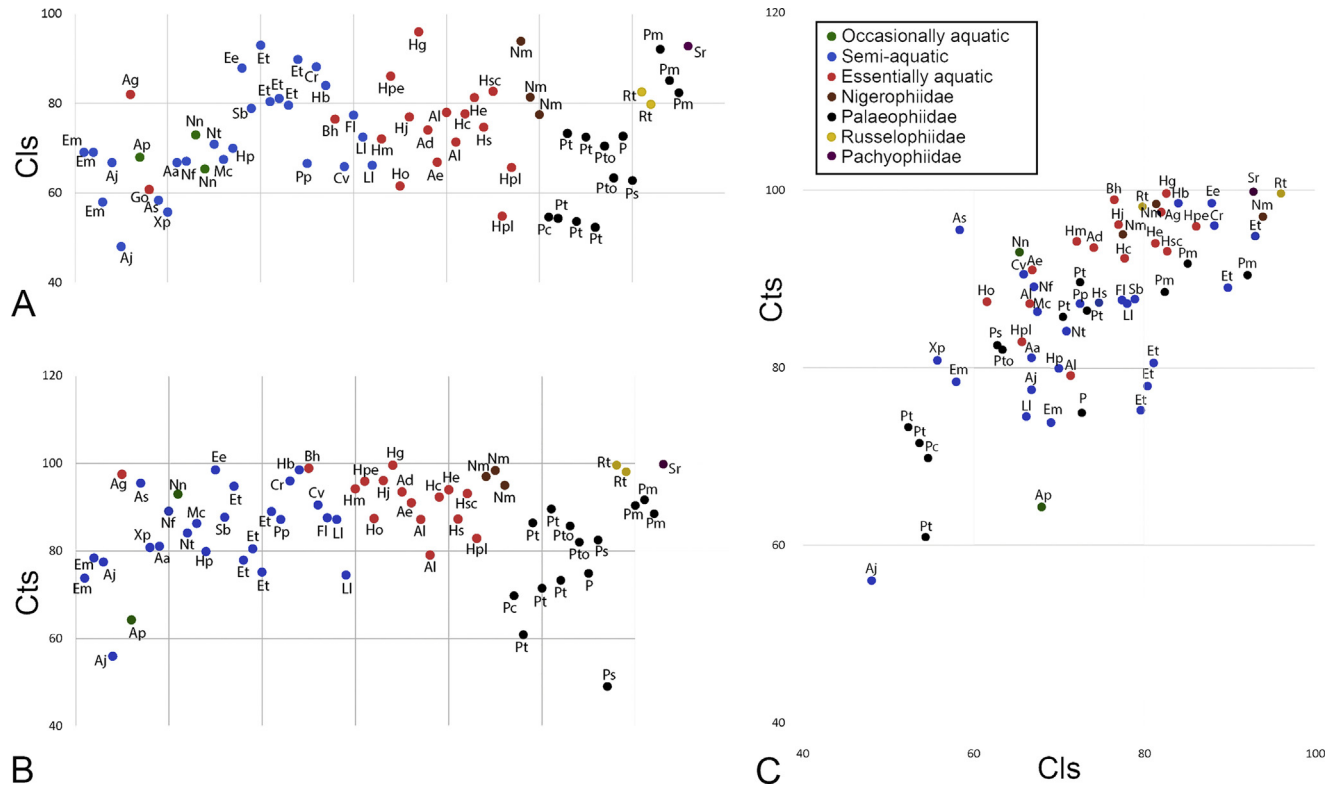


**Fig. 14.** Graphs illustrating the compactness values for our sample with color indications for the various ecologies and the family of the extinct taxa. A. CIs values. B. Cts values. C. Their covariation. Species name abbreviations are listed in Tables 1 and 2.

**Fig. 14.** Graphiques illustrant les valeurs de compacité de notre échantillonnage avec des indications de couleur pour les différentes écologies et la famille des taxons éteints. A. Valeurs CIs. B. Valeurs Cts. C. Leur covariation. Les abréviations des noms d'espèces sont listées dans les Tableaux 1 et 2.

allow us to conclude on the amount and extent of calcified cartilage remains. Osteosclerosis has been described in the anterior and mid-precloacal regions in *Palaeophis maghrebianus*, though compactness is not extreme, based on the combination of an inhibition of primary bone (but not calcified cartilage) resorption with excessive secondary bone deposits during remodelling (Houssaye et al., 2013b). The other *Palaeophis* vertebrae show compactness values that do not suggest osteosclerosis. Different processes relative to cartilage and bone resorption/remodelling are thus encountered within these aquatic snakes. If primary bone resorption is limited in all compact vertebrae, the inhibition of calcified cartilage resorption and excessive secondary bone deposits during remodelling occur only in some taxa.

Snake vertebrae (whatever the ecology) are rather compact, as compared to those of other amniotes. The small sample of non-aquatic and non-flying amniotes from Houssaye et al. (2014) shows average *C<sub>i</sub>* and *C<sub>t</sub>* values of 43.4 and 45.9%, respectively, as compared to the 71.3 and 76.5% values obtained for terrestrial and arboreal squamates, excluding fossorial taxa that would increase these numbers. It has been emphasized that snakes generally display no clear microanatomical specialization in their vertebrae (neither in their ribs; Canoville et al., 2016), except a few ecologically highly specialized taxa (Houssaye et al., 2013a). Their generalist inner morphology was interpreted as resulting from their general use of different habitats and locomotor modes and the necessity for snakes to move efficiently in different environments. Bone mass increase could nevertheless be expected in aquatic taxa with extremely limited terrestrial locomotion and utilizing a single environment. Houssaye et al. (2013a) indeed suggested the occurrence of osteosclerosis in *Erpeton tentaculatum*, which usually remains suspended or anchored to vegetation while hunting in rather shallow water (Smith et al., 2002) and, to a lesser extent, in *Enhydryis bocourti*. Conversely to these taxa confined to a single milieu, *Laticauda* moves in both deep water and across land, which could explain the absence of bone mass increase in this taxon. As for surface swimmers not requiring buoyancy control, like *Hydrophis platurus*, the absence of bone mass increase was expected. The addition of numerous semi-aquatic and marine taxa to the sample from Houssaye et al. (2013a) enables a wider comparative analysis. Our results show no strong difference in snake vertebral compactness between an aquatic lifestyle and the other ecologies. It also highlights a high variation in compactness for both semi-aquatic and aquatic snakes with no distinction between the two habitat preferences.

Therefore, no good correlation is highlighted between the compactness values and the ecology in snake vertebrae. It is not possible to assume an aquatic lifestyle based on high compactness, as for other amniotes (e.g., Amson et al., 2015; Buffrénil et al., 2010; Hayashi et al., 2013; Houssaye et al., 2016). Among aquatic forms, which occupy a great diversity of habitats, compactness also does not enable to distinguish the various ecologies. This comparative analysis thus shows that it is not possible to make reliable palaeoecological inferences for snakes based on vertebral microanatomy, although this tool appears very efficient for other amniotes and/or other bones (e.g.,

Dumont et al., 2013; Houssaye and Botton-Divet, 2018; Laurin et al., 2011). This result is all the more surprising because snakes do not have limbs and the axial skeleton is thus more strongly involved in locomotion as compared to limbed-amniotes. However, as previously suggested, snakes seem to display a rather generalist vertebral inner structure (Buffrénil and Rage, 1993; Houssaye et al., 2013a). Osteosclerosis needs to be determined based on the relative condition in “non-affected” sister taxa. Compactness being rather high in numerous snakes, this prevents the use of the term osteosclerosis in the most compact bones. The peculiarity of snakes strongly raises the question of the characterization of osteosclerosis: should it be based on a compactness threshold or on a mechanism? Our comparative analysis highlights the extreme difficulty in finding a threshold value. As for the mechanism, the few taxa for which classical sections were available show different processes of bone mass increase, with inhibition or enhancement of different processes. The use of the term “osteosclerosis” appears thus extremely complex and ambiguous for snakes.

### 5.3. The peculiarity of the marine hind-limbed snakes

One group remains peculiar among snakes: the marine hind-limbed snakes. These Cenomanian snakes are the only snakes displaying pachyostosis. It occurs in all trunk vertebrae and ribs except the anteriormost and posteriormost ones, with a maximal intensity in the mid-trunk region (see Houssaye, 2013 for a review on this question). This osseous specialization is intense in these taxa, though less strong in smaller specimens within each species (as observed in *Eupodophis*, *Pachyrhachis*, and *Pachyophis*; Houssaye, 2013).

Bone mass increase is considered to enable an increase in oxygen store and to control buoyancy and body trim (Taylor, 2000). Though more intense in the mid-trunk region, bone mass increase seems to affect almost the entire vertebral column in pachyophiids (Houssaye et al., 2011), which suggests a limited, if present, role in body trim control. In marine snakes, oxygen store is likely not a problem, since they can absorb oxygen through their skin. Other morphological features, e.g., cardiac shuntage, increase in blood volume, the sacular lung, are also suggested to increase immersion duration in snakes (Heatwole, 1999; Ineich, 2004). But cutaneous respiration is considered one major adaptation of sea snakes to a marine lifestyle (Heatwole, 1999) and is limited to these taxa within squamates. There is currently no consensus about the status and phylogenetic position of the pachyophiids (Caldwell, 2000; Martill et al., 2015; Palci et al., 2013b; Reeder et al., 2015; Rieppel and Zaher, 2000). If pachyophiids are among the first snakes, they might not show the morphological specializations observed in other sea snakes, notably cutaneous respiration, which might explain the need for strong bone mass increase in order to increase oxygen store. Compactness in most snakes is often rather high. The occurrence of pachyostosis might be a mean to further increase bone mass. The combination of osteosclerosis and pachyostosis (pachyosteosclerosis) is similarly observed in the precloacal skeleton of some “dolichosaurs” or stem-ophidians that



display a morphology rather similar to that of hind-limbed snakes (elongated skeleton with a high number of vertebrae and a reduction of the limbs) and are supposed to have lived in similar environments as the pachyophiids, i.e. coastal shallow waters (Houssaye, 2013). Pachyostosis is assumed to reduce movements between adjacent vertebrae and might have caused a reduction in lateral undulation in these taxa, whose aquatic locomotion might have thus slightly differed from that of other snakes.

## 6. Conclusion

The description of the inner structure of vertebrae of various extinct aquatic snakes and the interpretation of these microanatomical data in the light of a large comparative sample of extant snakes shows:

- important intraspecific variation in the vertebral microstructure in some snake taxa;
- that the vertebral microstructure cannot be used as a reliable ecological proxy in snakes, even for specialized species;
- that the use of the term “osteosclerosis” in snakes is extremely complex;
- the peculiarity of marine hind-limbed snakes that are the sole snakes showing pachyostosis.

## Acknowledgments

We would like to thank M. Lemoine and P. Loubry (MNHN, Paris, France) for the making of the thin sections and vertebra pictures, respectively. We are thankful to G.V.R. Prasad (University of Delhi, India) and B. Marandat (ISEM, Montpellier, France) for the loan of the *Indophis* and *Nigerophis* vertebrae, respectively, and V. de Buffrénil (MNHN, Paris, France) for the loan of the *P. colossaeus* sections. We thank K. Lim (Lee Kong Chian Natural History Museum, Singapore) for loaning us extant material for scanning. We thank the Steinmann Institute (University of Bonn, Germany), R. Lebrun (ISEM, Montpellier, France) and the MRI platform member of the national infrastructure France-BioImaging (supported by the ANR-10-INBS-04, “Investments for the future”, the labex CEMEB [ANR-10-LABX-0004] and NUMEV [ANR-10-LABX-0020]), the “Centre de microtomographie” of the Université de Poitiers, P. Tafforeau and the beamline ID19 of the ESRF (Grenoble, France), for providing access, beamtime, and support. This research did not receive any specific grant from funding agencies in the public, commercial, or not-for-profit sectors. This manuscript is naturally dedicated to the memory of Jean-Claude who supervised part of this work during the Ph.D. thesis of A. Ho. To the memory of a wonderful and inspiring scientist!

## References

Abramoff, M.D., Magelhaes, P.J., Ram, S.J., 2004. [Image processing with ImageJ](#). *Biophoton Int.* 11, 36–42.

Amson, E., Argot, C., McDonald, H.G., de Muizon, C., 2015. [Osteology and Functional Morphology of the Forelimb of the Marine Sloth \*Thalassocnus\* \(Mammalia, Tardigrada\)](#). *J. Mamm. Evol.* 22, 169–242.

Arambourg, C., 1952. [Les vertébrés fossiles des gisements de phosphates \(Maroc–Algérie–Tunisie\)](#). *Notes Mem. Serv. Geol. Maroc* 92, 1–372.

Aubret, F., Shine, R., 2008. [The origin of evolutionary innovations: locomotor consequences of tail shape in aquatic snakes](#). *Funct. Ecol.* 22, 317–322.

Auffenberg, W., 1959. [Anomalophis bolcensis \(Massalongo\), a new genus of fossil snake from the Italian Eocene](#). *Harvard Museum of Comparative Zoology. Breviora* 114, 1–16.

Babonis, L.S., Brischoux, F., 2012. [Perspectives on the convergent evolution of tetrapod salt glands](#). *Integr. Comp. Biol.* 52, 245–256.

Buffrénil, V.de., Rage, J.-C., 1993. [La « pachyostose » vertébrale de \*Simoliophis\* \(Reptilia, Squamata\) : données comparatives et considérations fonctionnelles](#). *Ann. Paleontol.* 79, 315–335.

Buffrénil, V.de., Bardet, N., Pereda-Suberbiola, X., Bouya, B., 2008. [Specialization of bone structure in \*Pachyvaranus crassispodylus\* Arambourg, 1952, an aquatic squamate from the Late Cretaceous of the southern Tethyan margin](#). *Lethaia* 41, 59–69.

Buffrénil, V.de., Canoville, A., D’Anastasio, R., Domning, D.P., 2010. [Evolution of Sirenian pachyosteosclerosis, a model-case for the study of bone structure in aquatic tetrapods](#). *J. Mammal. Evol.* 17, 101–120.

Caldwell, M.W., 2000. [On the phylogenetic relationships of \*Pachyrhachis\* within snakes: a response to Zaher \(1998\)](#). *J. Vert. Paleontol.* 20, 187–190.

Canoville, A., Buffrénil, V., Laurin, M., 2016. [Microanatomical diversity of amniote ribs: an exploratory quantitative study](#). *Biol. J. Linn. Soc.* 118, 706–733.

Das, I., 2015. [A Field Guide to the Reptiles of South-East Asia](#). New Holland Publishers, London, UK.

Dumont, M., Laurin, M., Jacques, F., Pelle, E., Dabin, W., de Buffrénil, V., 2013. [Inner architecture of vertebral centra in terrestrial and aquatic mammals: a two-dimensional comparative study](#). *J. Morphol.* 274, 570–584.

Figueroa, A., McKelvy, A.D., Grismer, L.L., Bell, C.D., Lailvaux, S.P., 2016. [A species-level phylogeny of extant snakes with description of a new colubrid subfamily and genus](#). *Plos One* 11, e0161070.

Gibbons, J.W., Dorcas, M.E., 2004. [North American Watersnakes: A Natural History](#). University of Oklahoma Press, Norman, OK, USA.

Hayashi, S., Houssaye, A., Nakajima, Y., Chiba, K., Ando, T., Sawamura, H., Inuzuka, N., Kaneko, N., Osaki, T., 2013. [Bone inner structure suggests increasing aquatic adaptations in \*Desmostylia\* \(Mammalia, Afrotheria\)](#). *Plos One* 8, e59146.

Heatwole, H., 1999. [Sea Snakes](#). New South Wales Press Ltd, Sydney, Australia.

Houssaye, A., 2009. [“Pachyostosis” in aquatic amniotes: a review](#). *Integr. Zool.* 4, 325–340.

Houssaye, A., 2013. [Palaeoecological and morphofunctional interpretation of bone mass increase: an example in Late Cretaceous shallow marine squamates](#). *Biol. Rev.* 88, 117–139.

Houssaye, A., Boistel, R., Böhme, W., Herrel, A., 2013a. [Jack-of-all-trades master of all? Snake vertebrae have a generalist inner organization](#). *Naturwissenschaften* 100, 997–1006.

Houssaye, A., Botton-Divet, L., 2018. [From land to water: evolutionary changes in long bone microanatomy of otters \(Mammalia: Mustelidae\)](#). *Biol. J. Linn. Soc.* 125, 240–249.

Houssaye, A., Buffrénil, V. de, Rage, J.-C., Bardet, N., 2008. [An analysis of vertebral ‘pachyostosis’ in \*Carentonosaurus mineaui\* \(Mosasauroida, Squamata\) from the Cenomanian \(early Late Cretaceous\) of France, with comments on its phylogenetic and functional significance](#). *J. Vert. Paleontol.* 28, 685–691.

Houssaye, A., Martin Sander, P., Klein, N., 2016. [Adaptive patterns in aquatic amniote bone microanatomy—More complex than previously thought](#). *Integr. Comp. Biol.* 56, 1349–1369.

Houssaye, A., Mazurier, A., Herrel, A., Volpato, V., Tafforeau, P., Boistel, R., Buffrénil, V. de, 2010. [Vertebral microanatomy in squamates: structure, growth and ecological correlates](#). *J. Anat.* 217, 715–727.

Houssaye, A., Rage, J.-C., Bardet, N., Vincent, P., Amaghaz, M., Meslouh, S., 2013b. [New highlights about the enigmatic marine snake \*Palaeophis maghrebianus\* \(Palaeophiidae; Palaeophiinae\) from the Ypresian \(Lower Eocene\) phosphates of Morocco](#). *Palaeontology* 56, 647–661.

Houssaye, A., Tafforeau, P., Herrel, A., 2014. [Amniote vertebral microanatomy – what are the major trends?](#) *Biol. J. Linn. Soc.* 112, 735–746.

Houssaye, A., Xu, F., Helfen, L., Buffrénil, V. de, Baumbach, T., Tafforeau, P., 2011. [Three-dimensional pelvis and limb anatomy of the Cenomanian hind-limbed snake \*Eupodophis descouensi\* \(Squamata, Ophidia\) revealed by synchrotron-radiation computed laminography](#). *J. Vert. Paleontol.* 31, 2–7.

- Hutchison, J.H., 1985. *Pterosphenus* cf. *P. scucherti* Lucas (Squamata, Palaeophidae) from the Late Eocene of Peninsular Florida. *J. Vert. Paleontol.* 5, 20–23.
- Ineich, I., 2004. Les serpents marins. Institut océanographique, Paris (320 p.).
- Ineich, I., Laboute, P., 2002. Les serpents marins de Nouvelle-Calédonie. Muséum national d'histoire Naturelle, Paris, France.
- Laurin, M., Canoville, A., Germain, D., 2011. Bone microanatomy and lifestyle: a descriptive approach. *C. R. Palevol* 10, 381–402.
- Lee, M.S.Y., Caldwell, M.W., Scanlon, J.D., 1999. A second primitive marine snake: *Pachyophis woodwardi* from the Cretaceous of Bosnia-Herzegovina. *J. Zool. Lond.* 248, 509–520.
- Lucas, F.A., 1899. A new snake from the Eocene of Alabama. *US Natl. Mus. Proc.* 21, 637–638.
- Martill, D.M., Tischlinger, H., Longrich, N.R., 2015. A four-legged snake from the Early Cretaceous of Gondwana. *Science* 349, 416–419.
- Murphy, J.C., 2007. Homalopsid Snakes. Evolution in the Mud. Krieger Publishing Company, Malabar, Florida (249 p.).
- Owen, R., 1841. Description of some ophiolites (*Paleophis toliapicus*) from the London Clay of Sheppey, indicating an extinct species of serpent. *Trans. Geol. Soc., 2nd. Ser.* 6, 209.
- Owen, R., 1850. Monograph on the fossil Reptilia of the London Clay. Part III. Ophidia. *Palaeontogr. Soc.* 3, 51–68.
- Palci, A., Caldwell, M.W., Albino, A.M., 2013a. Emended diagnosis and phylogenetic relationships of the Upper Cretaceous fossil snake *Najash rionegrina* Apesteguía and Zaher, 2006. *J. Vert. Paleontol.* 33, 131–140.
- Palci, A., Caldwell, M.W., Nydam, R.L., 2013b. Reevaluation of the anatomy of the Cenomanian (Upper Cretaceous) hind-limbed marine fossil snakes *Pachyrhachis*, *Haasiophis*, and *Eupodophis*. *J. Vert. Paleontol.* 33, 1328–1342.
- Parmley, D., DeVore, M., 2005. Palaeopheid snakes from the Late Eocene Hardie Mine local fauna of central Georgia. *Southeastern Nat.* 4, 703–722.
- Pauwels, O.S., Vande Weghe, J., 2008. Reptiles du Gabon. Smithsonian Institution, Washington DC, USA (272 p.).
- Rage, J.-C., 1975a. Un serpent du Paléocène du Niger. Étude préliminaire sur l'origine des Caenophidiens (Reptilia, Serpentes). *C. R. Acad. Sci. Paris, Ser. D* 281, 515–518.
- Rage, J.-C., 1975b. Un Caenophidien primitif (Reptilia, Serpentes) dans l'Eocène inférieur. *C. R. somm. Soc. geol. Fr. Paris* 2, 46–47.
- Rage, J.-C., 1983a. *Palaeophis colossaeus* nov. sp. (le plus grand serpent connu ?) de l'Eocène du Mali et le problème du genre chez les Palaeopheinae. *C. R. Acad. Sci. Paris, Ser. III* 296, 1029–1032.
- Rage, J.-C., 1983b. Les serpents aquatiques de l'Éocène européen. Définition des espèces et aspects stratigraphiques. *Bull. Mus. natn. Hist. nat.* 2, 213–241.
- Rage, J.-C., 1984. Handbuch der Paläoherpetologie, Teil 11. Serpentes. Gustav Fischer Verlag, Stuttgart/New York.
- Rage, J.-C., Prasad, G.V.R., 1992. New snakes from the late Cretaceous (Maastrichtian) of Naskal, India. *N. Jb. Geol. Palaeont. Abh.* 187, 83–97.
- Rage, J.-C., Prasad, G.V.R., Bajpai, S., 2004. Additional snakes from the uppermost Cretaceous (Maastrichtian) of India. *Cretaceous Res.* 25, 425–434.
- Rage, J.-C., Werner, C., 1999. Mid-Cretaceous (Cenomanian) snakes from Wadi Abu Hashim, Sudan: the earliest snake assemblage. *Paleont. Afr.* 35, 85–110.
- Rage, J.-C., Bajpai, S., Thewissen, J.G.M., Tiwari, B.N., 2003. Early Eocene snakes from Kutch, Western India, with a review of the Palaeophiidae. *Geodiversitas* 25, 695–716.
- Reeder, T.W., Townsend, T.M., Mulcahy, D.G., Noonan, B.P., Wood Jr., P.L., Sites Jr., J.W., Wiens, J.J., 2015. Integrated analyses resolve conflicts over Squamate reptile phylogeny and reveal unexpected placements for fossil taxa. *Plos One* 10, e0118199.
- Ricqlès, A. de, Buffrénil, V. de, 2001. Bone histology, heterochronies and the return of tetrapods to life in water: where are we? In: Mazin, J.-M., Buffrénil, V. de (Eds.), Secondary Adaptation of Tetrapods to Life in Water. Verlag Dr. Friedrich Pfeil, Munich, Germany, pp. 289–310.
- Rieppel, O., Zaher, H., 2000. The braincases of mosasaurs and *Varanus*, and the relationships of snakes. *Zool. J. Linn. Soc.* 129, 489–514.
- Segall, M., Cornette, R., Fabre, A.-C., Godoy-Diana, R., Herrel, A., 2016. Does aquatic foraging impact head shape evolution in snakes? *Proc. Roy. Soc. B – Biol. Sci.* 283, 20161645.
- Segall, M., Herrel, A., Godoy-Diana, R., 2019. Hydrodynamics of frontal striking in aquatic snakes: drag, added mass, and the possible consequences for prey capture success. *Bioinspir. Biomim.* 14, 036005.
- Smith, T.L., Povel, G.D.E., Kardong, K.V., 2002. Predatory strike of the tentacled snake (*Erpeton tentaculatum*). *J. Zool.* 256, 233–242.
- Taylor, M.A., 2000. Functional significance of bone ballast in the evolution of buoyancy control strategies by aquatic tetrapods. *Hist. Biol.* 14, 15–31.
- Welch, B.L., 1947. The generalization of 'Student's' problem when several different population variances are involved. *Biometrika* 34, 28–35.
- Westgate, J.W., Ward, J.F., 1981. The giant aquatic snake *Pterosphenus schucherti* (Palaeophidae) in Arkansas and Mississippi. *J. Vert. Paleontol.* 1, 161–164.